Steady-State Tokamak Discharge via dc Helicity Injection

M. Ono, G. J. Greene, D. Darrow, C. Forest, H. Park, and T. H. Stix
Princeton Plasma Physics Laboratory, Princeton University, Princeton, New Jersey 08544
(Received 18 May 1987)

A tokamak discharge has been formed and maintained through helicity injection, by use of only an external dc low-energy electron beam. The discharge, in a 5-kG toroidal field, evolved to a steady-state circular cross section with $q(a)=10$, $q(0)=4$, which was maintained for more than 400 L/R periods, the time (60 msec) limited by the cathode bias supply. The density profile reached a line-averaged $\bar{n}_e=2\times10^{13}$ cm^{-3}, while $T_e=25$ eV and $T_i=15$ eV. Strong central peaking occurs and inward pinching is indicated for *both* density and current.

PACS numbers: 52.80.Sm, 52.50.Gj, 52.55.Fa

In order to drive plasma current in a tokamak, it is necessary to inject "helicity" into the plasma (helicity is a quantity closely related to the amount of current in the plasma).[1] Inductive Ohmic current drive and noninductive rf current drive[2] are the two major approaches now used for helicity injection into tokamak plasmas. However, the former method is inherently not steady state, and the efficiency of the latter may not be high enough for reactor applications.[3] Recently, other types of helicity injection have been proposed.[4-8] These new ideas, often referred to as "dc" and "ac" helicity injection, may lead to more efficient methods for driving steady-state current and for controlling the current profile,[9] both of which are crucial for an economic tokamak reactor.

A small toroidal facility, CDX, is dedicated to the study of helicity injection based on the nonclassical behavior of radial current diffusion.[7,10] In the present experiment, the CDX helicity source is a steady-state low-energy electron beam which produces a current sheath at the surface of the toroidal plasma. The current is then transported radially inward by nonclassical processes. The ultimate current-drive efficiency for a low-energy beam can be quite good, theoretically approaching Ohmic-drive efficiency within a factor of 10.[11]

For both dc and ac helicity-injection schemes, current is generated near the plasma edge and, to be useful, must subsequently be transported into the interior of the plasma in order to offset resistive current decay. This process conceptually requires a nonclassical mechanism for current diffusion such as a current-profile–dependent instability.[7] As an example, a strong edge current is expected to trigger the double-tearing instability only if its direction of flow is parallel to that of the interior current. Magnetic turbulence associated with the instability could then facilitate rapid radial penetration of the edge current.[12,13] Spheromak experiments have already demonstrated the formation of a spheromak plasma with the dc helicity-injection concept, although on shorter time scales.[14] In this Letter, we report the first demonstration of formation and maintenance of a steady-state tokamak discharge via dc helicity injection and we present evidence for strong inward current transport.

The CDX machine is a toroidal magnetic-confinement device with major and minor radii of 59 and 10 cm, respectively, and a steady-state on-axis field of 5 kG. The vacuum vessel, toroidal field coils, and power supplies are composed of the former Advanced Concepts Torus-1.[15] Major modifications including the addition of internal coils, high-current electron-beam injectors, and new diagnostics have provided a machine specialized for the study of helicity-injection current drive, and the facility is now designated CDX (Current Drive Experiment).

Plasma is created in the CDX device by injection of an electron beam from a cathode at the bottom of the machine, Fig. 1. The cathode consists of lanthanum hex-

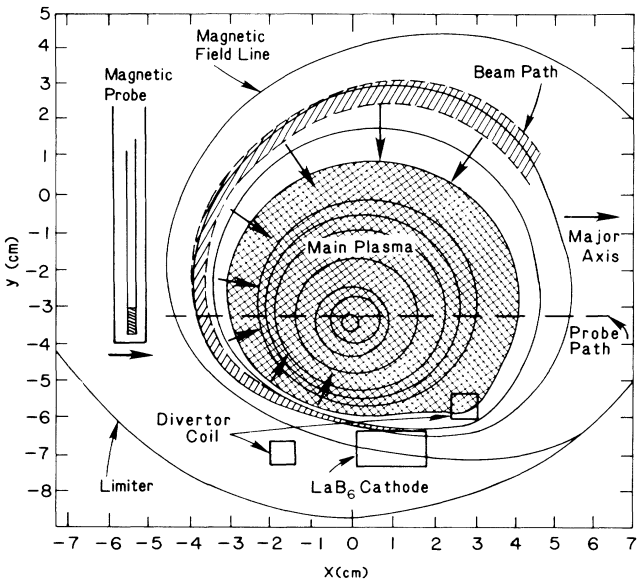

FIG. 1. Poloidal cross section for the dc helicity-injection experiment. Magnetic field contours computed by a 2D numerical simulation code. The lightly shaded area shows the electron beam path, and the darker shaded area indicates a region of closed magnetic field lines. The total toroidal plasma current, I_T, is 330 A.

aboride (LaB_6) tubes, about 1 cm in diameter and 1 cm in length, placed over electrically heated carbon rods; LaB_6 was utilized for its high emissivity at relatively low temperature.[16-18] The cathode is biased with respect to the limiter and chamber wall, and in vacuum the electron beam spirals gently upward, following the magnetic field lines. The vacuum poloidal field, Fig. 2, is strong near the divertor coils (7–10 G), Figs. 1 and 2, and enables the electron beam to avoid the cathode as it travels upward. As the beam drifts into the main plasma region, the vacuum poloidal field then decreases rapidly and is typically $\simeq 2$ G at the plasma center.

To model the experiment, a two-dimensional current-transport code was developed. It computes the toroidal current on a grid, I_{ij}, according to the following equation:

$$\partial I_{ij}/\partial t = -I_{ij}/\tau_{ij} - \nabla\cdot(D_{ij}\nabla I_{ij}) - \nabla\cdot(I_{ij}\mathbf{V}_{ij}) + S_{ij}. \quad (1)$$

The terms on the right-hand side of the equation represent plasma resistivity, current diffusion,[10] pinching, and injected-current source terms, respectively. The diffusion and pinching coefficients, which are nonclassical in nature, are chosen to match the experimental observations. In this regard, the simulation is similar to the approaches taken by the tokamak transport codes[19] for analysis of anomalous transport processes. The source term is nonzero only for those grid points which lie in the path of the injected electron beam current. It is assumed that electrons emitted from the cathode follow single-particle trajectories for a single 90° scattering distance. For simplicity, we have assumed spatially uniform resistivity, diffusion, and pinching coefficients. (This assumption may be reasonable for a small tokamak plasma where the electron temperature tends to be relatively uniform.) When current diffuses out of the plasma boundary (hitting the limiters), it is considered to be lost. The code advances in units of the plasma resistive time until a steady-state solution is reached. Accordingly, we normalize the diffusion and pinching coefficients to the resistivity time, minimizing the error due to uncertainty of the plasma resistivity.

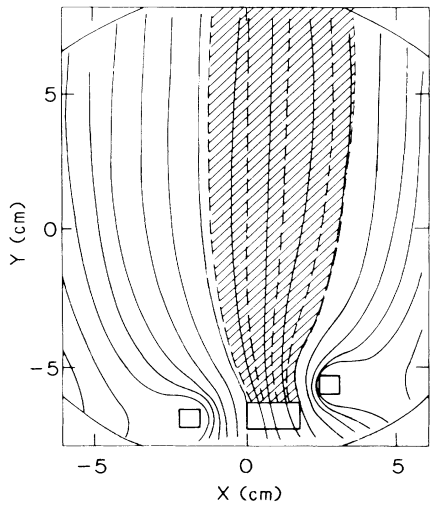

FIG. 2. Magnetic field contours for the vacuum poloidal field, $I_T = 10$ A.

Figure 2 shows the poloidal field configuration when the injected current is still sufficiently low that the vacuum poloidal field dictates the electron beam path. When the injected current has increased sufficiently that the self-generated poloidal fields dominate the vacuum poloidal fields, a dramatic change in the magnetic field structure takes place, shown in Fig. 1. In this configuration, the injected electron beam circulates around the main current-carrying plasma while helicity associated with the beam is transferred to the main plasma which now displays a field structure similar to that of a conventional tokamak. Laboratory confirmation of this computed tokamak configuration was a major goal of the experiments described here.

The experiments were conducted with hydrogen or helium as a working gas, at a typical prefill pressure of 3×10^{-4} Torr. The LaB_6 cathodes were heated continuously, and the discharge was created entirely by the electron beam, pulsing the cathode bias for 30–60 msec. The cathode bias voltage, typically 300 V, produced injected electron-gun currents up to $\simeq 50$ A, and the discharge could be repeated at a rate of 2–4 Hz.

Time-resolved images of the discharge formation obtained with photographic sampling with use of an electro-optic shutter[20] ("boxcar photography") displayed a tokamaklike circular structure similar to the corresponding computed cases. The minor radius of the steady-state discharge inferred from the photograph is about 3 cm, and the resulting safety factor, q, at the plasma edge is $\simeq 10$. When the cathode bias was pulsed off, the plasma current decayed with an L/R time typically $\tau_{res} \simeq 130$ μsec. On the assumption of a 1.2-μH inductance for the 3-cm radius current channel, the implied space-averaged conductivity temperature is $kT_e \simeq 25$ eV for the estimated $Z_{eff} \simeq 1.5$. The high-current discharge was maintained for over 400 resistive time periods, its duration limited by the capacity of the cathode bias supply.

A special water-cooled radially scanning magnetic probe was developed to measure the generated poloidal magnetic field. Magnetic-flux diffusion through the probe structure is rapid compared to the time scales of interest, and the probe signal was processed through a low-noise, high-gain integrator to yield an output proportional to the magnetic field linking the coil. The midplane poloidal magnetic field for the steady-state plasma is shown in Fig. 3. As expected, the poloidal field reverses near the center of the discharge. The measured

poloidal field at the plasma edge of 20–25 G (much larger than the vacuum poloidal field of $\simeq 2$ G) was consistent with the plasma current of 330 A (measured with an internal electrostatically shielded Rogowski coil) and the observed discharge radius of 3 cm (on the assumption of circular symmetry). The field was typically 10%–15% larger on the small major radius side, consistent with the toroidal geometry. The current density and q profile obtained from this measurement, $q=(B_t/B_p)(r/R)$, are shown in the inset of Fig. 3. q decreases monotonically with the plasma radius, from $q=10$ at the edge to $q=4$ at the center, and the centrally peaked current profile is somewhat surprising in that the current source in this experiment is purely external.

A comparison of the experimental measurements with the simulation shows the presence of very strong current diffusion and an inward current pinch. In order to produce the circular discharge shown in Fig. 1, it was necessary in our code to use current-diffusion and pinch terms of $D_j \approx 4$ cm$^2/\tau_{\rm res}$ and $V_j \approx 12$ cm$/\tau_{\rm res}$. This indication of anomalous current penetration may be related to recent theoretical investigations in which an anomalous current diffusion was obtained,[8,21] driven by a resistive MHD instability.

One can estimate the experimental helicity-injection efficiency using the helicity equation in steady state,[5]

$$\epsilon \int 2\Phi \mathbf{B}\cdot\mathbf{n}\,dS = -\int 2\eta \mathbf{j}\cdot\mathbf{B}\,dV, \qquad (2)$$

where the left-hand term is the rate of helicity injection and the right-hand term is the resistive loss term. Here, Φ is the relative potential between cathode and plasma, η is the plasma resistivity, and j is the current density. We define here an experimental helicity-injection efficiency coefficient as ϵ. Equation (2) can be reduced to $\epsilon\Phi B_v \Delta A = IB_T\bar{\eta}2\pi R$, where ΔA is the effective cathode area of $\simeq$(1 cm)$\times 2\pi R$, B_V is the vertical field strength near cathode of $\simeq 10$ G, $B_T - 4.3$ kG, $I=330$ A, $R=59$ cm, and $\bar{\eta}$ is the average plasma resistivity. From Eq. (2), we obtain $\epsilon \simeq 0.5$ or about 50% efficiency of the dc helicity injection in our experiment.

The density measured in the high-current, tokamak-like discharge by the dual-beam far-infrared laser interferometer[22] is shown in Fig. 4. High plasma density is seen within 3 to 4 cm of the plasma axis. The central chord-averaged density is $\bar{n}_e = 2\times 10^{13}$ cm^{-3} with a fall-off length of 3–4 cm. The steep profile suggests good particle confinement in this tokamak regime. Average ion temperatures, determined by the Doppler broadening of the He II λ 4686 line increased from $\simeq 1$ eV in the low-current discharge to $\simeq 15$ eV in the tokamak discharge.

In conclusion, a tokamak plasma configuration has been created and maintained in steady state for the first time by means of dc helicity injection via a low-energy electron beam. As the plasma current increased, a circular discharge evolved which was qualitatively similar to the predictions of a numerical code that invoked both current diffusion and current pinching. The poloidal magnetic field measurements demonstrated a centrally peaked current profile with q values ranging from 10 at the edge to 4 near the center. In addition, a highly peaked plasma density profile with central chord-averaged values of 2×10^{13} cm^{-3} was observed, and average ion and electron temperatures were approximately 15 and 25 eV, respectively. Preparations are now underway to increase the plasma current to the 1-kA range which corresponds to $q(a)=4$ discharge in an

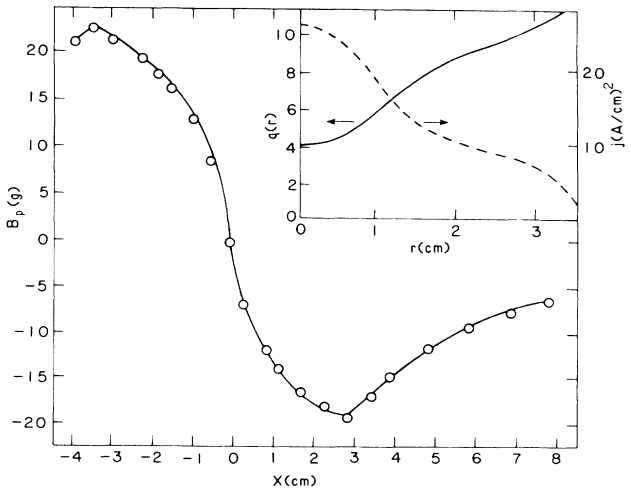

FIG. 3. Midplane poloidal magnetic field as a function of radial position. $I_T=330$ A, $B_0=4.5$ kG, and $R_0=59$ cm. Inset: Corresponding deduced q and j values as a function of the minor radius.

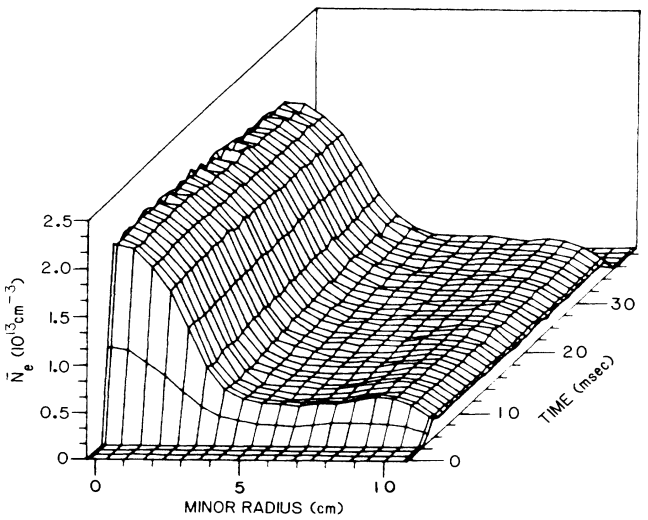

FIG. 4. Temporal evolution of the vertical chord-averaged density as a function of radial position, $r=R-R_0$, where R_0 is the major radius of the plasma axis.

Ohmic-driven tokamak plasma on CDX.

The authors thank J. Taylor and W. Kineyko for their excellent technical support. We thank H. Furth and K. Bol for useful suggestions and support. We also thank J. R. Wilson for technical suggestions and helpful discussions. One of the authors (M.O.) appreciated contributions from J. Bowman, H. Okuda, and S. Jardin in the development of the 2D simulation code. Special thanks are due to D. McNeill for his advice on the Doppler broadening measurements. This work is supported by U.S. Department of Energy Contract No. DE-AC02-76CHO3073.

[1]J. B. Taylor, Phys. Rev. Lett. **33**, 1139 (1974).

[2]N. J. Fisch, Phys. Rev. Lett. **41**, 873 (1978).

[3]C. Karney and N. J. Fisch, Phys. Fluids **28**, 116 (1985).

[4]M. K. Bevir and J. W. Gray, Los Alamos National Laboratory Report No. LA-8944-C, 1981 (unpublished), p. 176; M. K. Bevir, C. G. Gimblett, and G. Miller, Phys. Fluids **28**, 1826 (1985).

[5]T. H. Jensen and M. S. Chu, Phys. Fluids **27**, 2881 (1984).

[6]P. M. Bellan, Phys. Rev. Lett. **54**, 1381 (1985).

[7]T. H. Stix and M. Ono, Princeton University Plasma Physics Laboratory Report No. PPPL-2211, 1985 (unpublished).

[8]J. M. Finn and T. M. Antonsen, Jr., University of Maryland Report No. UMLPF 86-031, 1986 (to be published).

[9]M. S. Chance, S. C. Jardin, and T. H. Stix, Phys. Rev. Lett. **51**, 1963 (1983).

[10]T. H. Stix, Nucl. Fusion **18**, 3 (1978).

[11]R. Armstrong *et al.*, Bull. Am. Phys. Soc. **30**, 1624 (1985).

[12]H. P. Furth, P. H. Rutherford, and H. Selberg, Phys. Fluids **16**, 1054 (1973).

[13]T. H. Stix, Phys. Rev. Lett. **36**, 521 (1976).

[14]T. R. Jarboe *et al.*, Phys. Rev. Lett. **51**, 39 (1983).

[15]K. L. Wong, M. Ono, and G. A. Wurden, Rev. Sci. Instrum. **53**, 409 (1982).

[16]D. M. Goebel, J. T. Grow, and A. T. Forrester, Rev. Sci. Instrum. **49**, 469 (1978).

[17]R. Horton, M. Ono, K. L. Wong, and H. Okuda, Bull. Am. Phys. Soc. **29**, 1367 (1984).

[18]H. Okuda, R. Horton, M. Ono, and K. L. Wong, Phys. Fluids **28**, 3365 (1986).

[19]C. Singer *et al.*, Princeton University Plasma Physics Laboratory Report No. PPPL-2037, 1983 (unpublished).

[20]G. Greene, G. Cutsogeorge, and M. Ono, Princeton University Plasma Physics Laboratory Report No. PPPL-2429, 1987 (to be published).

[21]M. Tanaka *et al.*, in Proceedings of the Eleventh Conference on Plasma Physics and Controlled Nuclear Fusion Research, Kyoto, Japan, 1986 (to be published), paper E-I-3.

[22]D. S. Darrow, M. Ono, and H. K. Park, Bull. Am. Phys. Soc. **31**, 1614 (1986).